Department of Pharmacology and Toxicology[1], Faculty of Pharmacy, South Valley University, Qena; Department of Pharmacology and Toxicology[2], Faculty of Pharmacy, Beni-Suef University, Beni-Suef; Department of Pathology and Clinical Pathology[3], Faculty of Veterinary Medicine, South Valley University, Qena, Egypt

Potential roles for eNOS and NrF_2/HO-1 signaling in the ameliorative effect of lixisenatide on diabetes-induced kidney injury in rats and its amplification by ticagrelor co-administration

M. Sleem[1,*], E. M. Aboubakr[1], W. R. Mohamed[2], A. M. Khalil[3], B. A. S. Messiha[2], A. Taye[1]

Received May 26, 2024, accepted July 1, 2024

**Corresponding author: Mostafa Sleem, Department of Pharmacology and Toxicology, Faculty of Pharmacy, South Valley University, Qena, 83523, Egypt*
mstfa_slm@svu.edu.eg

Pharmazie 79: 187-194 (2024) *doi: 10.1691/ph.2024.4566*

Antioxidant and anti-inflammatory effects of lixisenatide (LX) and ticagrelor (TC) have been previously identified in type 2 diabetes mellitus (T2DM). Diabetic nephropathy is one of the major complications of T2DM. In the current study, we examined the potential protective effects of LX and TC on experimentally induced diabetic nephropathy in T2DM rats and their possible molecular mechanisms. To examine this possibility, rats were fed a high-fat diet (HFD) for 12 weeks, followed by a single injection of 35 mg/kg streptozotocin (STZ) to induce T2DM. 10 µg/kg LX and 25 mg/kg TC were given alone or in combination to T2DM rats for 4 weeks. The kidney examination of T2DM rats showed clear deterioration. T2DM rats exhibited significantly higher body weight, blood glucose, hemostatic model assessment for insulin resistance (HOMA-IR), blood urea nitrogen (BUN), serum creatinine, kidney reactive oxygen species (ROS), nuclear factor-κB (NF-κB), and transforming growth factor-β (TGF-β), and significantly lower serum insulin, urine creatinine, creatinine clearance (CRCL), kidney superoxide dismutase (SOD), glutathione reduced (GSH), nuclear factor erythroid 2 (NrF_2), heme oxygenase-1 (HO-1), and endothelial nitric oxide synthase (eNOS) when compared to control rats. Single treatment with LX or TC showed obvious ameliorative effects on kidney complications in T2DM rats, with more ameliorative effects with the combined administration of both drugs. Conclusion: Our investigation found that both LX and TC could significantly ameliorate the development of diabetic nephropathy via stimulating NrF_2/HO-1 antioxidant pathway in addition to increasing eNOS and decreasing NF-κB renal tissue concentrations, and these effects were markedly augmented by their combined administration.

1. Introduction

Diabetic nephropathy is one of the most important renal complications associated with diabetes mellitus (DM) (Vincent et al. 2011). Changes in glucose homeostasis and altered metabolic status are strongly linked to type 2 diabetes mellitus (T2DM). The consequences of correlated abnormalities are reported to impair the function of numerous organs, such as the kidneys and cardiovascular system (Sleem et al. 2014). Functional and histological abnormalities in diabetic renal problems have been linked to a number of chronic hyperglycemia-triggered metabolic alterations, including elevated levels of advanced glycation end products (AGEs) and increased reactive oxygen species (ROS) (Yamagishi et al. 2007). Numerous findings imply that AGE buildup in the glomeruli may be related to the inflammatory fibrosis processes that occur in diabetic nephropathy (Yamagishi 2019). Diabetes promotes atherosclerosis and inflammation through the production of intracellular ROS and the additional role of consequent activation of the transcription factor nuclear factor-κB (NF-κB) (Yamagishi et al. 2008). NF-κB is a crucial transcription factor that could control several genes linked to inflammatory and immunological responses (Zhao et al. 2021). On the other hand, nuclear factor erythroid 2 (NrF_2) plays a crucial role in controlling the oxidative stress response. Moreover, downstream gene expression is involved in the NrF_2-mediated transcription process, which activates antioxidants enzymes including superoxide dismutase (SOD), glutathione reduced (GSH), and Heme oxygenase-1 (HO-1) (Cui et al. 2019). HO-1 has been shown to play a part in preventing vascular injury and may be one of the most significant defense mechanisms that is triggered during periods of cellular stress such as inflammation and enhanced oxidative stress (Abraham and Kappas 2008). NrF_2 and HO-1 are essential targets for the treatment of the renal and vascular consequences of DM, this signaling pathway is thought to be significant in oxidative stress responses and has been linked to other functions like apoptosis, antioxidants, and anti-inflammatory responses (Fiorelli et al. 2019). Despite the remarkable advancements in nephroprotective treatment of T2DM, renal replacement therapies are still required globally, and the frequency of this condition is rising, which necessitates the need for further studies and research (Ham et al. 2023).

Recently, there has been interest in using glucagon-like peptide-1 (GLP-1) as a treatment for DM and obesity. LX, an agonist of the GLP-1 receptor, has been suggested as a possible target for the treatment of individuals with T2DM because of its ability to increase glucose-induced insulin release from pancreatic β-cells, decrease glucagon secretion, and slow stomach emptying (Kuwata et al. 2021). LX may affect tissues outside the pancreas and cause a variety of physiologic reactions in the renal and cardiovascular systems (Seufert and Gallwitz 2014). Furthermore, LX consistently improves renal and cardiovascular events in animal models (Wohlfart et al. 2013; Abdel-Latif et al. 2020). Earlier research has indicated that LX has anti-inflammatory and anti-ROS characteristics, hence offering defense

Table 1: Effects of LX and TC on body weight, blood glucose, serum insulin, and HOMA-IR of rats with T2DM

Animal group / Parmeter.	C	D	D+LX	D+TC	D+LX+TC
Body weight (gm) Mean ± SEM	257 ± 16.85	361.5 ± 17.10 *	255.7 ± 14.76 #	340.8 ± 22.88 *	208.8 ± 13.18 #, $
Blood glucose (mg/dl) Mean ± SEM	82.78 ± 11.20	440.6 ± 18.71 *	189.8 ± 21.07 *, #	376.7 ± 20.33 *	166.3 ± 29.20 #, $
Insulin (µIU/mL) Mean ± SEM	13.44 ± 1.48	6.37 ± 0.89 *	10.35 ± 0.75 #	7.70 ± 0.70 *	10.85 ± 0.71 #
HOMA-IR Mean ± SEM	2.18 ± 0.47	7.35 ± 0.91 *	3.98 ± 0.54 #	6.73 ± 0.92 *	3.04 ± 0.45 #, $

Data represent mean±SEM (n=6). * Significant difference from C, # significant difference from D, and $ significant difference from D+TC at p<0.05. HOMA-IR: hemostatic model assessment for insulin resistance; C: Control; D: Diabetic; LX: lixisenatide; TC: ticagrelor.

against vascular damage in T2DM (Zhao et al. 2019). Furthermore, it was noted that LX might block NF-κB activation, which is brought on by free fatty acids in animal models (Zhao et al. 2019).

Ticagrelor (TC), a P2Y12 receptor antagonist, has been shown to reduce inflammatory indicators by inhibiting adenosine uptake (Armstrong et al. 2014). Prior research demonstrated that TC could have anti-fibrotic and anti-inflammatory properties (Ye et al. 2015). Furthermore, a study revealed that TC reduces apoptosis, shielding cells from oxidative stress responses (El-Mokadem et al. 2021). Additionally, an in vitro investigation found that TC stimulates endothelial eNOS in rats (Ariotti et al. 2018).

Therefore, the current study was carried out to investigate the potential protective effects of single and combined administration of LX and TC against diabetic nephropathy in experimentally induced T2DM in rats and the potential involvement of NrF_2/HO-1, eNOS, and NF-κB signaling in this effect.

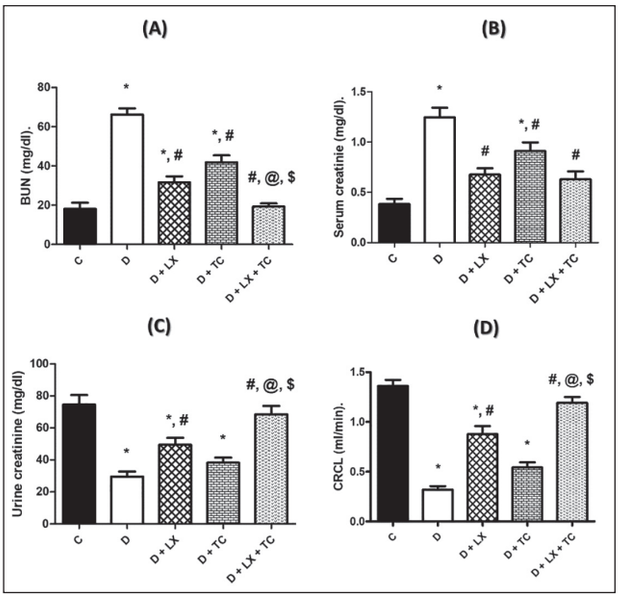

Fig. 1: Effects of LX and TC on BUN (A), serum creatinine (B), urine creatinine (C), and CRCL (D). Data represent mean±SEM (n=6). * Significant difference from C, # significant difference from D, @ significant difference from D+LX, and $ significant difference from D+TC at p<0.05. BUN: Blood urea nitrogen; CRCL: Creatinine clearance; C: Control; D: Diabetic; LX: lixisenatide; TC: ticagrelor.

2. Investigations and results

2.1. Effects of LX and TC on body weight, blood glucose, serum insulin, and the HOMA-IR index of rats with T2DM

Table 1 depicts the alterations in body weight, blood glucose, serum insulin, and HOMA-IR in T2DM rats after administering LX and TC separately and in combination. Body weight, blood glucose, and HOMA-IR data revealed a significant elevation, while serum insulin revealed a significant reduction in D compared to C. D+LX and D+LX+TC showed a significant reduction in body weight, blood glucose, and HOMA-IR, and significant elevation in serum insulin compared to D. While D+LX+TC showed a significant reduction in blood glucose, body weight, and HOMA-IR compared to D+TC.

2.2. Effects of LX and TC on BUN, serum creatinine, urine creatinine, and CRCL of rats with T2DM

Figure 1 (A-D) depicts the alterations in BUN, serum creatinine, urine creatinine, and CRCL in T2DM rats after administering LX and TC separately and in combination. BUN and serum creatinine showed significant elevation, while urine creatinine and CRCL showed significant reduction in D compared to C. Single and combined administration of LX and TC showed significant reduction in BUN and serum creatinine compared to D. Moreover, administration of LX and LX+TC showed significant elevation in urine creatinine and CRCL compared to D. Interestingly, administration of LX+TC showed a significant reduction in BUN and significant elevation in urine creatinine and CRCL compared to D+LX and D+TC groups.

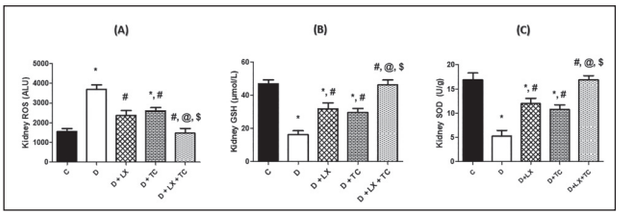

Fig. 2: Effects of LX and TC on kidney ROS (A), GSH (B), and SOD (C) of T2DM rats. Data represent the mean±SEM (n=6). * Significant difference from C, # significant difference from D, @ significant difference from D+LX, and $ significant difference from the D+TC at P<0.05. ROS: reactive oxygen species; SOD: superoxide dismutase; GSH: glutathione reduced. C: Control; D: Diabetic; LX: lixisenatide; TC: ticagrelor.

2.3. Effects of LX and TC on kidney ROS, GSH, and SOD of T2DM rats

Figure 2 (A-C) shows the changes in kidney ROS, GSH, and SOD in T2DM rats after administering LX and TC separately and in combination. Kidney ROS demonstrated a significant elevation, while kidney GSH and SOD demonstrated a significant reduction in D compared to C. Both single and combined administration of LX and TC demonstrated a significant reduction in ROS and a significant elevation in GSH and SOD compared to D. Interestingly, administration of LX+TC showed a significant reduction in ROS and a significant elevation in GSH and SOD compared to D+LX and D+TC.

2.4. Effects of LX and TC on kidney NrF_2, HO-1, eNOS, and NF-κB expression of T2DM rats

The renal NrF_2, HO-1, eNOS, and NF-κB changes in T2DM rats are shown in Figure 3 (A-E) following the administration of LX and TC alone and in combination. kidney NF-κB demonstrated a significant increase, but kidney NrF_2, HO-1, and eNOS demonstrated a significant decrease in D in contrast to C. Furthermore, in comparison to D, both the single and combined administration of LX and TC demonstrated a significant decrease in NF-κB and significant increase in NrF_2, HO-1, and eNOS. Additionally, compared to D+LX and D+TC, administration of LX+TC demonstrated a significant increase in NrF_2 and a significant drop in NF-κB. Also a significant increase in eNOS was noticed compared to D+TC.

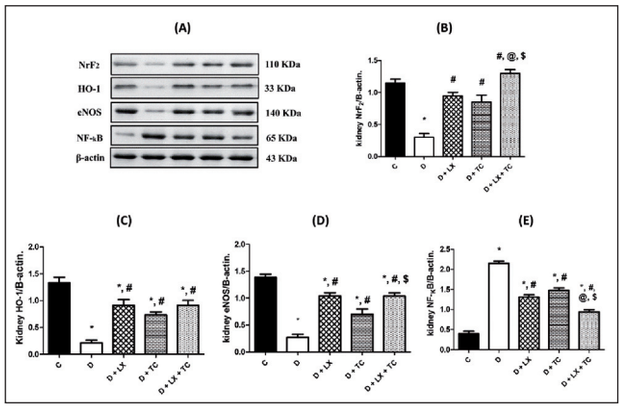

Fig. 3: Effects of LX and TC on kidney NrF_2 (B), HO-1 (C), eNOS (D), and NF-κB (E) of T2DM rats. Data represent (n=3) mean±SEM. * significant difference from the C, # significant difference from the D, @ significant difference from the D+LX, and $ significant difference from the D+TC at P<0.05. C: Control; D: Diabetic; LX: lixisenatide; TC: ticagrelor. NrF_2: nuclear factor erythroid-2; HO-1: heme oxygenase-1; eNOS: endothelial nitric oxide synthase; NF-κB: nuclear factor kappa B.

2.5. Effects of LX and TC on kidney TGF-β of T2DM rats.

Renal tissue sections were stained immunohistochemically to assess the expression of TGF-β in the different groups as shown in Figure 4 (A-F). Control group exhibited a negative TGF-β expression (Fig. 4A). In diabetic animals TGF-β was expressed highly in the renal glomeruli basement membrane, in Bowman's capsule, and around the renal tubules (Fig. 4B). Moreover, the expression was prominent around the affected renal arteries (Fig. 4C). The administration of LX caused a decrease in TGF-β expression which exhibited only as a rim on the Bowman's capsule membrane (Fig. 4D). Similar to LX, administration of TC decreased the expression of TGF-β which appeared only in mild percentage on renal glomeruli (Fig. 4E). Co-administration of both drugs exhibited no expression on the renal glomeruli and appeared only as low expression on the wall of renal blood supply (Fig. 4F).

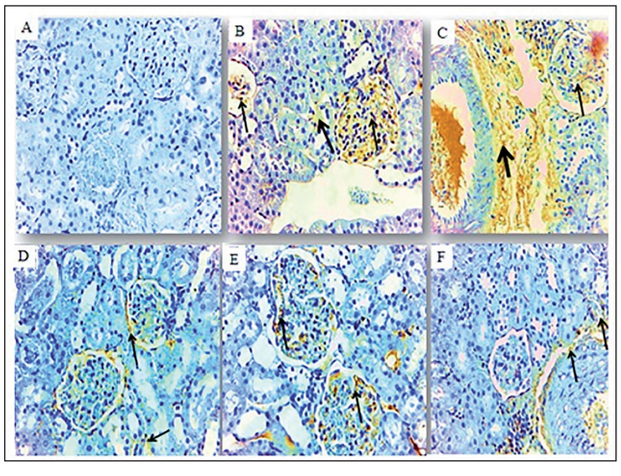

Fig. 4: Effects of LX and TC on kidney TGF-β of T2DM rats. Photomicrograph of renal tissues in rats stained immunohistochemically to assess the expression of TGF-β in the different groups. The control group exhibited a negative response to TGF-β expression (A). In diabetic animals, TGF-β was expressed highly in the renal glomeruli basement membrane and the Bowman's capsule (thin arrow) and around the renal tubules (thick arrow) (B). Moreover, the expression of the cytokine was prominent around the affected renal arteries (thick arrow) (C). Administration of LX caused a reduction in TGF-β expression which appeared only as a rim on the Bowman's capsule membrane (arrow) (D). Giving of TC decreased the expression of TGF-β which appeared in a mild percentage in the renal glomeruli (arrow) (E). Co-administration of both drugs exhibited no expression on the renal glomeruli and appeared only as a low expression on the wall of renal blood supply (arrow) (F), (400X).

2.6. Effects of LX and TC on kidney histopathological injury of T2DM rats

Histopathological damage was examined in renal sections stained with H&E stain are shown in Figure 5 (A-F). In the control rats the renal tissues microscopically appeared normal without noticed pathological changes in the renal glomeruli as well as the renal tubular epithelium and blood supply as shown in (Fig. 5A). In Diabetic rats a marked pathological change in the renal glomeruli and vasculature were reported which are manifested by mesangial expansion with thickening of the glomerular basement membrane associated with blood vessels congestion (Fig. 5B). In other tissue sections of diabetic rats' kidney, there was thickening in the wall of renal artery with blood clotting surrounded with inflammatory cell infiltration (Fig. 5C). LX administration to the diabetic rats exhibited improvement in renal tissue damage caused by high blood glucose as characterized by normal meningeal cells and Bowman's space dilatation, in addition to normal dilation of the renal tubules with mild hydropic degeneration (Fig. 5D). Similarly,

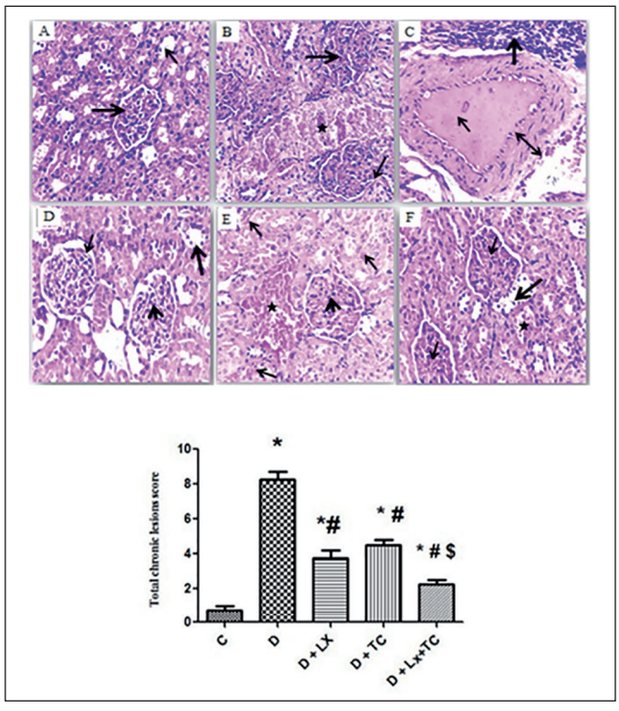

Fig. 5: Effects of LX and TC on kidney histopathological injury of T2DM rats. C, normal without pathological changes in the glomeruli (thick arrow) and renal epithelium (thin arrow) (A). D, mesangial expansion (thick arrow), thickening of the glomerulai (thin arrow), blood vessel congestion (star) (B). Thickening of renal artery (double head arrow), blood clotting (thin arrow), cell infiltration (thick arrow) (C). D+LX, normal mesangial cells (arrowhead), Bowman's space dilatation (thin arrow), normal dilation of the renal tubules with mild hydropic degeneration (thick arrow) (D). D+TC, decrease in mesangial cell proliferation (Arrowhead), increases in the blood supply in the renal tissue (arrows) and dilation to the renal artery (star) (E). D+LX+TC, normal epithelium (thin arrow) and normal tubular dilatation (thick arrow) and normal renal blood supply (star) (F). (400X). Data represent (n=4) mean±SEM. * significant from C, # significant from D, and $ significant from D+TC at P<0.05. C: Control; D: Diabetic; LX: lixisenatide; TC: ticagrelor.

treatment with TC counteracted the pathological changes caused by hyperglycemia as evidenced by a marked decrease in mesangial cell proliferation and expansion with increases in the blood supply flow in the renal tissues with dilation to the renal artery (Fig. 5D). Co-administration of LX and TC caused nearly complete recovery to the pathological damage induced in diabetic rats which was evidenced by normal glomerular epithelium and normal tubular dilatation as well as normal renal blood supply (Fig. 5F).

2.7. Effects of LX and TC on kidney fibrosis and collagen deposition

Staining of the renal sections was done with Masson's trichrome to assess the collagen fiber distribution in the different groups as shown in Figure 6 (A-F). No collagen fibers were spread in the renal tissues of C group (Fig. 6A). In D group there was elevated distribution of collagen fiber around the renal tubules and renal blood supply (Fig. 6B), as well as on the renal glomerular membranes (Fig. 6C). The administration of LX and TC individually exhibited very low distribution of the collagen fiber mainly around the renal tubules as shown in Fig 6 (D&E). D+LX+TC revealed normal renal tissues without collagen fiber distribution (Fig. 6F).

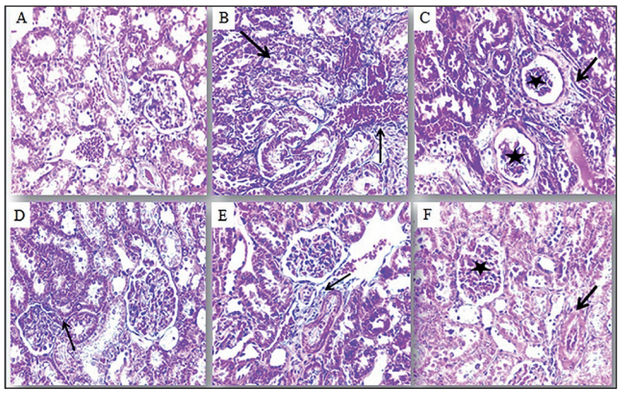

Fig. 6: Effects of LX and TC on kidney fibrosis and collagen deposition. Staining of renal sections with Masson's trichrome to assess collagen fiber distribution in different groups. No collagen fibers were spread in renal tissue of C group (A). In D group there was a high distribution of collagen fiber around the renal tubules and renal blood supply (arrow) (B), as well as renal glomerular membranes (star) (C). The administration of LX and TC individually exhibited very low distribution of the collagen fiber mainly around the renal tubules (arrow) (D&E). CO administration of LX and TC to diabetic rats revealed normal renal tissues without collagen fiber distribution (F), (400X).

3. Discussion

Individuals who have been exposed to T2DM for an extended period are more susceptible to cardiovascular and renal problems than other groups. Obesity, insulin resistance, hyperglycemia, and elevated ROS are the main metabolic disorders responsible for long-term cardiovascular changes in patients with T2DM (Rojas-Carranza et al. 2018; Maranta et al. 2021).

The current study looked at how the GLP-1 agonist; LX and the P_2Y_{12} inhibitor; TC can slow down or even reverse the metabolic and renal alterations brought on by T2DM, which in turn accelerates the development of diabetic nephropathy. Previous research showed that the pathophysiology of T2DM would be similar in rats fed HFD to cause peripheral insulin resistance, followed by low dosage of STZ to target pancreatic beta cells (Reed et al. 2000). In this study, in comparison to control the STZ-HFD-induced T2DM model showed a significant decrease in blood insulin levels and a significant increase in body weight, blood glucose, and HOMA-IR. Our study's findings were consistent with early publications which stated that obesity, insulin resistance, and hyperglycemia are attributed to the HFD's administration in growing female rats (Flanagan et al. 2008), while the injection of STZ can lower blood insulin levels in T2DM rats (Zhang et al. 2021).

Treatment with the medications under examination in the current study demonstrated that both single and combined administration of LX with TC led to a significant decrease in weight, blood glucose, and HOMA-IR of the animals, with a significant increase in insulin release when compared to diabetic rats. Conversely, single TC treatment did not seem to have any significant impact on body weight, blood glucose, HOMA-IR, or insulin release when compared to diabetic rats, which was in consistence with previous studies found that LX administration can stimulate insulin secretion from pancreatic beta cells in a glucose-dependent manner (Davis and Sandoval 2020). Besides, administration of LX showed significant reduction in HOMA-IR in T2DM patients (Fineman et al. 2012).

Serum and urine creatinine alongside BUN, are considered important factors for assessing kidney function in diabetic rats (Hogan et al. 2023). Also, CRCL is an important estimate for glomerular filtration rate and kidney function in diabetic patients (Rufino et al. 2007). In our study, diabetic rats' serum creatinine and BUN were significantly increased while urine creatinine and CRCL were significantly reduced compared to control rats.

Similar results were previously described that elevated serum creatinine and BUN, along with decreased excretion of creatinine in the urine, are common signs of diabetic nephropathy in diabetic mice (Song et al. 2020). Also, another study revealed a significant decrease in CRCL in DM rats (Al-Rasheed et al. 2018).

In this investigation, both single and combined treatments of LX and TC significantly reduced serum creatinine and BUN levels compared to untreated diabetic animals. Besides, single administration of LX and its co-administration with TC significantly increased urine creatinine and CRCL. It is interesting to note that using LX and TC combined administration could significantly produce higher amelioration than using either medication alone.

An imbalance between ROS and the antioxidant defense systems of cells is known as oxidative stress, It could be brought about in diabetic patients by changes in the metabolism of glucose or subsequent dysregulation of number of enzymes that are not directly engaged in glucose metabolism (Giugliano et al. 1996).

As previously reported from gene expression omnibus database, diabetic nephropathy is considered a consequence of elevated ROS production (Yuchen et al. 2023). Besides, excessive generation of ROS is among the common pathways related to disrupted renal hemodynamics in STZ diabetic rat kidney (Nankar et al. 2020).

In the current investigation, the kidney of diabetic rats showed a significant decrease in GSH and SOD and a significant rise in ROS. These results agreed with previous reports stating that in DM hyperglycemia increases the generation of ROS and decreases the activity of antioxidants as SOD and GSH leading to oxidative damage to different tissues in T2DM patients (Song et al. 2007). Also, early described in kidneys of diabetic rats, the antioxidant defense agents such as SOD and GSH were significantly reduced while ROS expression was enhanced (Baig et al. 2022).

Our research findings for the investigated medications demonstrated that a single administration of LX or TC to diabetic rats resulted in a significant decrease in kidney ROS and a significant rise in kidney GSH and SOD in comparison to diabetic untreated rats. It is interesting to note that when LX and TC were administered together, kidney ROS was significantly lower while GSH and SOD were significantly higher than when LX or TC were administered separately. These results are confirmed with reports stating that LX can induce a nephroprotective effect in T2DM rats through significant antioxidant effects as evidenced by a marked rise in total antioxidant capacity (Zhou et al. 2014).

A different study conducted on rats with doxorubicin-induced renal fibrosis revealed that giving LX dramatically restored the antioxidant capacity in renal fibrotic tissues and demonstrated a significant increase in GSH and SOD (Guo et al. 2019). On the other hand, recent studies in mice have reported that TC can attenuate the development of diabetic nephropathy (Birnbaum et al. 2022). Also, TC was reported to decrease hyperglycemia-induced ROS production and prevent the development of apoptosis in cardiomyocytes (Bitirim et al. 2022).

It was previously stated that activation of HO-1 through the action of NrF_2 can enhance the antioxidant protective effect in diabetic rats (Zhou et al. 2021). The protective benefits of HO-1 are seen during periods of cellular stress, such as inflammation. According to a recent human study, NrF_2 transcription and activation play a major part in HO-1 expression (Fiorelli et al. 2019). Moreover, the NrF_2/HO-1 pathway was able to inhibit NF-κB in animal models, which is considered a main inflammatory transcription factor (Ahmed et al. 2017). However, transcription factor NF-κB is charged with causing the release of several inflammatory molecules and causing vascular problems linked to DM in cell and animal-based experimental systems (Patel and Santani 2009). Moreover, collagen deposition and fibrosis in vascular tissues of STZ diabetic rats have also been linked to DM (Miric et al. 2001). Also, inflammatory molecules play an important role in DM and its associated complications *via* modulating NF-κB pathways in cells and animal models (Patel and Santani 2009). Moreover, activity of NF-κB is enhanced in hyperglycemic conditions in humans through the release of cytokines such as TGF-β, leading to cellular apoptosis and inflammatory processes (Evans and Goldfine 2016). As a result, enhanced TGF-β synthesis brought on by increased NF-κB activity in diabetic patients results in angiogenesis and injury to vascular cells (Kitada et al. 2010). Impairing eNOS function and activation of additional stress-induced apoptotic pathways was found in DM mice (Wang et al. 2019). In addition, previous reports indicated that reduced eNOS in vascular endothelial cells results in decreased NO production, which may exacerbate endothelial dysfunction in humans (Gliozzi et al. 2019). Our study results showed that NF-κB and TGF-β, as well as fibrosis and collagen deposition, were significantly enhanced in the kidneys of diabetic rats compared to controls, while NrF_2, HO-1, and eNOS levels were significantly decreased. Furthermore, there was a marked decline in the histological status of the kidneys of diabetic rats.

These findings corroborated a recent study that showed a significant decrease in HO-1, NrF_2, and eNOS in diabetic mice (Wang et al. 2020). Hyperglycemia in humans increases the presence of NF-κB, which was reported to cause endothelial cell death and inflammatory responses (Evans and Goldfine 2016). In addition, TGF-β expression is activated by ROS, which contributes to fibrosis and is considered a pathological characteristic of diabetic nephropathy in mice (Zhou et al. 2023). The current investigation found that in comparison to untreated diabetic rats both single and combined administration of LX and TC significantly increased NrF_2, HO-1, and eNOS while significantly decreased NF-κB and TGF-β, and collaged deposition with significant improvement in kidney histological condition. It's interesting to note that when LX and TC were administered together, there was a significant increase in NrF_2 and a significant decrease in NF-κB compared to drugs administered separately. However, there was also a significant increase in eNOS and a significant decrease in TGF-β, and collagen deposition compared to TC alone.

These results confirm previous reports where pretreatment with LX can increase both NrF_2 and HO-1, with enhanced eNOS phosphorylation and intracellular NO production in oxygen-glucose deprivation and reperfusion model (Xiao et al. 2020). Also, it was found that administration of LX through inhibition of NF-κB protects against doxorubicin-induced renal fibrosis in rats by TGF-β mediated pathways (Guo et al. 2023). Significant downregulation in renal expressions of TGF-β was also recorded in early-onset nephropathy in diabetic rats following treatment with LX (Abdel-Latif et al. 2020). On the other hand, TC was found to improve remodeling and reduce apoptosis, inflammation, and fibrosis in a rat model of ischemia-reperfusion (Birnbaum et al. 2019). Also, a study stated that TC enhanced the content of the NrF_2/HO-1 axis in the renal ischemia-reperfusion rat model (El-Mokadem et al. 2021). Moreover. TC effects on rats were reported to reduce ROS generation and enhance eNOS phosphorylation, leading to increased production of NO (Wang et al. 2018). Furthermore, an in vitro study on rats stated that TC may provoke adenosine-related effects including anti-inflammatory effects (Armstrong et al. 2014).

In conclusion, our study provides evidence for the efficacy of single and combined administration of LX and TC in attenuating T2DM-induced renal injury and related renal function impairment. Our data suggested the contribution of eNOS and NrF_2/HO-1 signaling and its downstream NF-κB, ROS, SOD, and GSH in the protective effect against T2DM renal complications. The combination of LX and TC exerted a more significant effect than their single use. However, further clinical studies need to be performed to investigate the clinical efficacy and effective dose regimen.

4. Experimental

4.1. Preparation of HFD and induction of T2DM

Powdered normal pellet diet (N.P.D) 1000 g, fat 531 g, casein 125 g, dl methionine 3 g, vitamin mix 7 g, and mineral mix 42 g were employed in the preparation of HFD (about 40% of calories from fat) (Gheibi et al. 2017). After 12 weeks of feeding HFD, a single intraperitoneal injection of 35 mg/kg of STZ (Solar Bio® Life Science, Beijing) dissolved in citrate buffer was administered to rats. Rats were tested after three days to identify diabetic animals, defined as those whose fasting blood glucose level was more than 200 mg/dl (Li et al. 2023). Casein and dl methionine were supplied by Sigma Aldrich, Germany. Tween 80, N.P.D., mineral mix, and vitamin mix were supplied by the South Valley University (SVU) lab.

4.2. Animals and experimental design

Fifty male Sprague Dawley rats, weighing between 120 and 170 g, were provided from the National Research Center in Cairo. Animal handling was performed following SVU ethical approval committee number, P.S.V.U. 011/22. Animals were housed in standard environmental conditions with a 14:10 hour light/dark cycle and free access to food and drink, except for the 12-hour fasting period before blood sample collection. The following groups (n = 6) were created: **(C)**: nondiabetic control group, received normal fat baseline diet for 12 weeks followed by single intraperitoneal (i.p.) injection of citrate buffer. **(D)**: nondrug-treated diabetic group, diabetes was induced by receiving high-fat diet (HFD) for 12 weeks followed by a single i.p. injection of Streptozotocin (STZ) (35 mg/kg) dissolved in citrate buffer. **(D+LX)**: diabetic rats treated with LX (Sigma Aldrich, Germany) (10 µg/kg/day/S.C) dissolved in water for injection (Wohlfart et al. 2013). **(D+TC)**: diabetic rats treated with TC (RAMEDA, Egypt) (25 mg/kg/day/orally) dissolved in Tween 80 (Moustafa Ahmed et al. 2019). **(D+LX+TC)**: diabetic rats treated with LX+TC in the same doses. Drug treatment continues for 4 weeks for all groups (Jeric et al. 2015).

4.3. Urine, serum, and tissue sampling

Following a 12-hour fast, the animals were weighed, and a glucometer was used to assess their blood glucose levels. A 24-hour urine volume collection was used to determine urine creatinine content. Blood was drawn from the retroorbital veins of animals, and serum insulin, serum creatinine, and BUN levels were determined (Huang and Chen 2022). At the end of the experiment, isoflurane inhalation was used to induce anesthesia for tissue sampling (Bhatia et al. 2022). Each animal's kidney was removed, cleaned with a physiological solution, and then separated into three sections. One section was stored in 10% formalin for histopathological and immunostaining examination. Another section was stored in lysis buffer for western blot analysis. The third section was homogenized using cold Krebs-HEPES buffer with the following ingredients: 10 mmol/l glucose, 0.02 mmol/l Ca-Tri triplex, 25 mmol/l $NaHCO_3$, 1.2 mmol/l KH_2PO_4, 120 mmol/l NaCl, 1.6 mmol/l $CaCl_2{\cdot}2H_2O$, 1.2 mmol/l $MgSO_4{\cdot}$7H2O, and 5 mmol/l KCl. The pH of the buffer was 7.4 to measure kidney SOD, GSH, and ROS (Ertik et al. 2024).

4.4. Assessment of biomarkers

4.4.1. Body weight

Using a standard laboratory animal weight balance (RADWAG, Model: PS 2100.R2, UK), the animals' body weight was determined.

4.4.2. Blood glucose levels

Using Tango® TD-4235 glucometer, Taiwan, blood glucose level was determined in blood samples obtained from rat tails.

4.4.3. Serum insulin levels

The assay was conducted using an enzyme-linked immune-sorbent assay (ELISA) kit for rats, Fine Test, cat#: ER1113, China. In accordance with the manufacturing protocol, the quantity of insulin in the sample was correlated with the density of the yellow color at 450 nm (Kato et al. 1977).

4.4.4. Blood urea nitrogen (BUN)

Using BUN assay kit cat#: UR 2110, Bio Diagnostic, Egypt, ammonium ions formed were measured by the Berthelot reaction. The blue dye indophenol product reaction absorbs light between 530 nm and 560 nm and color intensity is proportional to the initial urea concentration (Wilcox et al. 1966).

4.4.5. Serum and urine creatinine

Using creatinine assay kit cat#: CR 1250, Bio Diagnostic, Egypt, serum creatinine was measured where it forms a colored complex with picrate in alkaline medium. Concentrations in the sample were measured at 520 nm (Schirmeister et al. 1964).

4.4.6. HOMA-IR estimation

HOMA-IR was calculated as follows:
HOMA-IR = [fasting glucose (mmol/L) × fasting insulin (μU/mL)]/22.5 (Bian et al. 2023).

4.4.7. CRCL estimation

The following equation was used to calculate CRCL.
CRCL (ml/min) = (urine creatinine X 24-h urine volume) / (serum creatinine X 1440). (Abdel-Wahab et al. 2018).

4.4.8. Kidney SOD

The suppression of pyrogallol autoxidation, which is directly related to the activity of SOD, was used to determine the SOD content of kidney tissue (Flohe and Otting 1984) using SOD assay kit cat#: SD 2521, Bio Diagnostic, Egypt.

4.4.9. Kidney GSH

Based on the reduction of Ellman's reagent [5, 5'-dithio-bis (2-nitrobenzoic acid)], the reduced glutathione concentration in the kidney was identified using GSH assay kit cat#: GR 2511, Bio Diagnostic, Egypt. Using spectrophotometry, the yellow color of nitro mercaptobenzoic acid can be measured at 412 nm (Ellman 1959).

4.4.10. Kidney ROS

Lucigenin 5 μmol/l (Sigma Aldrich, Germany) was used to assess superoxide generation after 20 min of incubation. NADPH 100 μmol/l (Sigma Aldrich, Germany) was added to initiate the reaction, and over the course of 30 min, the relative light units of chemiluminescence were determined. The results were adjusted for each sample's protein concentration (Brehm et al. 1996).

4.4.11. Western blot for kidney eNOS, NrF_2, HO-1, and NF-κB

Using a previously established protocol, kidney tissues were homogenized in Tris lysis buffer (400 mM NaCl, 0.5% Triton X-100, and 50 mM Tris at pH 7.4) with a protease inhibitor cocktail (BIOSPES, China) at 4 °C for 30 min (Henry et al. 1986). The remaining tissue was separated using centrifugation at 10,000 g for 10 min at 4 °C. The Biuret method was used to measure the concentrations of proteins (Wang et al. 1996). Equal protein amounts (30 μg) of total protein loaded in each lane were resolved using 10% sodium dodecyl sulfate-polyacrylamide gel electrophoresis and transferred to a polyvinylidene fluoride membrane (Millipore, Merk, USA) by methods of semi-dry transfer (Towbin et al. 1979). Tris-buffered saline containing 5% non-fat milk in Tween (TBST) buffer was used to block membranes for one hour at room temperature. This was followed by overnight incubation at 4 °C with primary antibodies. Subsequently, an alkaline phosphatase-conjugated secondary antibody (BIOSPES, China), was incubated on the membranes for an hour. The BCIP/NBT substrate detection kit (GENEMED, Biotechnologies, USA) was used to visualize the bands. National Institutes of Health, Bethesda, USA, imageJ® program was used to examine the bands that were created.
Antibodies used for western blot analysis include anti-NrF_2 cat#YPA1865, and anti-HO-1 cat#YPA1919, (BIOSPES, Chongqing). Anti-NF-κB cat#abx012874, (Abbexa, UK). anti-eNOS cat#sc-136977 (SANTA CRUZ BIOTECHNOLOGY, INC, USA). β-actin cat# E-AB-20031 (ELABSCIENCE, USA).
Dilutions of antibodies utilized are as follows: 1:5000 for the alkaline phosphatase-conjugated secondary antibody (Biospes, China), 1:3000 for the anti-β-actin antibody, and 1:2000 for the primary antibody.

4.4.12. Histopathological examination and immunostaining analysis

Kidneys were harvested and washed directly by phosphate buffer saline then fixed in 10 % neutral buffered formalin. The trimmed sections of kidney were passed in ascending series of alcohol 70 %, 80 %, 90%, and 100 %. The sections were then cleared in xylene and embedded in melted paraffin wax at 60 °C. Paraffin blocks were cut by microtome into 3 μm thin sections. Some of the prepared slides were stained by Hematoxylin and Eosin (H&E) (Levdik 1989). Masson trichrome staining was applied to 3 μm thick sections from every block to examine collagen fiber distribution (Goodman and Bernstein 1977). Sections with a thickness of 3 μm were placed on positive slides and used for immunohistochemical examination using primary anti-TGF-β antibody (cat#: EPR21143, ABCAM, USA). Samples were counterstained for 30 seconds with hematoxylin before being dehydrated and mounted (Taylor and Burns 1974). Slides were evaluated by an experienced pathologist, and imaging was done with a German LEICA Microsystems DM750 ICC50 W.
Renal tissue-stained sections were scored and evaluated according to previously documented scoring system (Sethi et al. 2017). Chronic changes were evaluated including the changes in the renal cortex and medulla; however, we were interested in the renal cortex due to the presence of glomeruli, tubules, interstitium, and arteries/arterioles. The evaluation included global and segmental glomerulosclerosis (GS) and tubular atrophy (TA) in addition to interstitial fibrosis (IF). In GS, glomerular capillary walls were examined. In TA, tubular shrinkage, thickening of the tubular basement membrane as well as the flattening of the tubular epithelium were evaluated. In interstitial fibrosis, the presence of fibrous tissues in between the tubules and glomerular wall was measured. Obtained data were judged as shown in Table 2. The resulting scoring and upcoming grading of the chronic damage were presented as follows: GS was scored from 0 to 3, TA from 0 to 3 and IF from 0 to 3. The issued scores were summed to obtain the total renal chronicity score which classifies the overall severity of the chronic lesions into minimal (0 –1 total score), mild (2 – 4 total score), moderate (5–7 total score), and severe (over than 8 total score).

Table 2: Scoring of the chronic lesions % in renal tissues

Tissues compartment	Score			
	0	1	2	3
GS score	<10%	10–25%	26%–50%	>50%
IF score	<10%	10–25%	26%–50%	>50%
TA score	<10%	10–25%	26%–50%	>50%

GS: Glomerulosclerosis; IF: interstitial fibrosis; TA: Tubular atrophy.

4.4.13. Statistical analysis

The data were analyzed using one-way analysis of variance (ANOVA) to check for statistically significant differences, and the Tukey-Kramer post-analysis test was used to compare all groups. The results are shown as means ± standard error of the mean (SEM). A *p*-value less than 0.05 was deemed to be significant. Statistical calculations were conducted using GraphPad Prism® Version 5.00 for Windows, Graph Pad Software, San Diego, California.

Author contribution: AT, BA and WR designed the research study. EM and MS performed the research and analyzed the data. AM examined histopathology and immune staining procedures. All authors contributed to editorial changes in the manuscript. All authors read and approved the final manuscript. All authors have participated sufficiently in the work and agreed to be accountable for all aspects of the work.

Availability of data and materials: All data in this study are available upon request by contacting the corresponding author.

Ethics, approval, and consent to participate: Animals were handled, and procedures were conducted following SVU's ethical approval committee number: P.S.V.U. 011/22.

Funding: No funding.

Conflicts of interest: The authors have no conflicts of interest to declare.

Acknowledgments: We would like to thank Dr. Fares Ali, Pharmacology and Toxicology Lecturer at Al-Azhar University, Assiut, Egypt. For his valuable contribution to western blot analysis.

References

Abdel-Latif RG, Ahmed AF, Heeba GH (2020) Low-dose lixisenatide protects against early-onset nephropathy induced in diabetic rats. Life Sci 263: 118592.
Abdel-Wahab AF, Bamagous GA, Al-Harizy RM, ElSawy NA, Shahzad N, Ibrahim IA, Ghamdi SSA (2018) Renal protective effect of SGLT2 inhibitor dapagliflozin alone and in combination with irbesartan in a rat model of diabetic nephropathy. Biomed Pharmacother 103: 59–66.
Abraham NG, Kappas A (2008) Pharmacological and clinical aspects of heme oxygenase. Pharmacol Rev 60: 79–127.
Ahmed SM, Luo L,Namani A, Wang XJ, Tang X (2017) Nrf2 signaling pathway: Pivotal roles in inflammation. Biochim Biophys Acta Mol Basis Dis 1863: 585–597.
Al-Rasheed NM, Al-Rasheed NM, Bassiouni YA, Hasan IH, Al-Amin MA, Al-Ajmi HN, Mahmoud AM (2018) Simvastatin ameliorates diabetic nephropathy by attenuating oxidative stress and apoptosis in a rat model of streptozotocin-induced type 1 diabetes. Biomed Pharmacother 105: 290–298.
Ariotti S, Ortega-Paz L, van Leeuwen M, Brugaletta S, Leonardi S, Akkerhuis KM, Rimoldi SF, Janssens G, Gianni U, van den Berge JC, Karagiannis A, Windecker S, Valgimigli M (2018) Effects of ticagrelor, prasugrel, or clopidogrel on endothelial function and other vascular viomarkers: A randomized crossover study. JACC Cardiovasc Interv 11: 1576– 1586.
Armstrong D, Summers C, Ewart L, Nylander S, Sidaway JE, van Giezen JJ (2014) Characterization of the adenosine pharmacology of ticagrelor reveals therapeutically relevant inhibition of equilibrative nucleoside transporter 1. J Cardiovasc Pharmacol Ther 19: 209–219.
Baig N, Sultan R, Qureshi SA (2022) Antioxidant and anti-inflammatory activities of Centratherum anthelminticum (L.) Kuntze seed oil in diabetic nephropathy via modulation of Nrf-2/HO-1 and NF-kappaB pathway. BMC Complement Med Ther 22: 301.
Bhatia A, Saikia PP, Dkhar B, Pyngrope H (2022) Anesthesia protocol for ear surgery in Wistar rats (animal research). Animal Model Exp Med 5: 183–188.
Bian L, Zhou Y, Zhang D, Jiang T, Xing C, Wu X, Wang T, Zhu X (2023) Negative correlation between serum pyruvate kinase M2 and cognitive function in patients with cerebral small vessel disease. Clin Neurol Neurosurg 225: 107586.

Birnbaum Y, Chen H, Tran D, Nylander S, Ye Y (2022) Ticagrelor and dapagliflozin have additive effects in ameliorating diabetic nephropathy in mice with type-2 diabetes mellitus. Cardiovasc Drugs Ther 36: 829–840.

Birnbaum Y, Tran D, Chen H, Nylander S, Sampaio LC, Ye Y (2019) Ticagrelor improves remodeling, reduces apoptosis, inflammation and fibrosis and increases the number of progenitor stem cells after myocardial infarction in a rat model of ischemia reperfusion. Cell Physiol Biochem 53: 961–981.

Bitirim CV, Ozer ZB, Aydos D, Genc K, Demirsoy S, Akcali KC, Turan B (202) Cardioprotective effect of extracellular vesicles derived from ticagrelor-pretreated cardiomyocyte on hyperglycemic cardiomyocytes through alleviation of oxidative and endoplasmic reticulum stress. Sci Rep 12: 5651.

Brehm M, Schiller E, Zeller WJ (1996) Quantification of reactive oxygen species generated by alveolar macrophages using lucigenin-enhanced chemiluminescence--methodical aspects. Toxicol Lett 87: 131–138.

Cui W, Leng B, Wang G (2019) Klotho protein inhibits H(2)O(2)-induced oxidative injury in endothelial cells via regulation of PI3K/AKT/Nrf2/HO-1 pathways. Can J Physiol Pharmacol 97: 370–376.

Davis EM, Sandoval DA (2020) Glucagon-like peptide-1: actions and influence on pancreatic hormone function. Compr Physiol 10: 577–595.

El-Mokadem BM, El-Abhar HS, Abdallah DM, Awad AS, Soubh AA (2021) Epac-1/Rap-1 signaling pathway orchestrates the reno-therapeutic effect of ticagrelor against renal ischemia/reperfusion model. Biomed Pharmacother 139: 111488.

Ellman GL (1959) Tissue sulfhydryl groups. Arch Biochem Biophys 82: 70–77.

Ertik O, Tunali S, Acar ET, Bal-Demirci T, Ulkuseven B, Yanardag R (2024) Antioxidant activity and protective effects of an oxovanadium (IV) complex on heart and aorta injury of STZ-diabetic rats. Biol Trace Elem Res 202: 2085-2099.

Evans JL, Goldfine ID (2016) A new road for treating the vascular complications of diabetes: So let's step on the gas. Diabetes 65: 346–348.

Fineman MS, Cirincione BB, Maggs D, Diamant M (2012) GLP-1 based therapies: differential effects on fasting and postprandial glucose. Diabetes Obes Metab 14: 675–688.

Fiorelli S, Porro B, Cosentino N, Di Minno A, Manega CM, Fabbiocchi F, Niccoli G, Fracassi F, Barbieri S, Marenzi G, Crea F, Cavalca V, Tremoli E, Eligini S (2019) Activation of Nrf2/HO-1 pathway and human atherosclerotic plaque vulnerability: an in vitro and in vivo study. Cells 8: 356.

Flanagan AM, Brown JL, Santiago CA, Aad PY, Spicer LJ, Spicer MT (2008) High-fat diets promote insulin resistance through cytokine gene expression in growing female rats. J Nutr Biochem 19: 505–513.

Flohe L, Otting F (1984) Superoxide dismutase assays. Methods Enzymol 105: 93–104.

Gheibi S, Bakhtiarzadeh F, Jeddi S, Farrokhfall K, Zardooz H, Ghasemi A (2017) Nitrite increases glucose-stimulated insulin secretion and islet insulin content in obese type 2 diabetic male rats. Nitric Oxide 64: 39–51.

Giugliano D, Ceriello A, Paolisso G (1996) Oxidative stress and diabetic vascular complications. Diabetes Care 19: 257–267.

Gliozzi M, Scicchitano M, Bosco F, Musolino V, Carresi C, Scarano F, Maiuolo J, Nucera S, Maretta A, Paone S, Mollace R, Ruga S, Zito MC, Macri R, Oppedisano F, Palma E, Salvemini D, Muscoli C, Mollace V (2019) Modulation of nitric oxide synthases by oxidized LDLs: role in vascular inflammation and atherosclerosis development. Int J Mol Sci 20: 3294.

Goodman PA, Bernstein J (1977) Better histopathologic technique. Arch Pathol Lab Med 101: 271–272.

Guo NF, Cao YJ, Chen X, Zhang Y, Fan YP, Liu J, Chen XL (2019) Lixisenatide protects doxorubicin-induced renal fibrosis by activating wNF-kappaB/TNF-alpha and TGF-beta/Smad pathways. Eur Rev Med Pharmacol Sci 23: 4017–4026.

Guo NF, Cao YJ, Chen X, Zhang Y, Fan YP, Liu J, Chen XL (2023) Retraction note: lixisenatide protects doxorubicin-induced renal fibrosis by activating wNF-kappaB/TNF-alpha and TGF-beta/Smad pathways. Eur Rev Med Pharmacol Sci 27: 6472.

Ham YR, Lee EJ, Kim HR, Jeon JW, Na KR, Lee KW, Choi DE (2023) Ultrasound renal score to predict the renal disease prognosis in patients with diabetic kidney disease: an investigative study. Diagnostics (Basel) 13: 515.

Henry RP, Dodgson SJ, Forster RE, Storey BT (1986) Rat lung carbonic anhydrase: activity, localization, and isozymes. J Appl Physiol 60: 638–645.

Hogan IA, Kuo YC, Abubakar AN, Lawal B, Agboola AR, Lukman HY, Onikanni SA, Olawale F, Fadaka AO, Ibrahim YO, Babalola SB, Batiha GE, Albogami SM, Alorabi M, De Waard M, Huang HS (2023) Attenuation of hyperglycemia-associated dyslipidemic, oxidative, cognitive, and inflammatory crises via modulation of neuronal ChEs/NF-kappaB/COX-2/NOx, and hepatorenal functional deficits by the Tridax procumbens extract. Biomed Pharmacother 158: 114114.

Huang YC, Chen BH (2022) A comparative study on improving streptozotocin-induced type 2 diabetes in rats by hydrosol, extract and nanoemulsion prepared from Cinnamon leaves. Antioxidants (Basel) 12: 29.)

Jeric M, Vuica A, Boric M, Puljak L, Jelicic Kadic A, Grkovic I, Filipovic N (2015) Diabetes mellitus affects activity of calcium/calmodulin-dependent protein kinase II alpha in rat trigeminal ganglia. J Chem Neuroanat 64-65: 12-19.

Kato K, Hamaguchi Y, Okawa S, Ishikawa E, Kobayashi K (1977) Use of rabbit antiboty IgG bound onto plain and aminoalkylsilyl glass surface for the enzyme-linked sandwich immunoassay. J Biochem 82: 261–266.

Kitada M, Zhang Z, Mima A, King GL (2010) Molecular mechanisms of diabetic vascular complications. J Diabetes Investig 1: 77–89.

Kuwata H, Yabe D, Murotani K, Fujiwara Y, Haraguchi T, Kubota S, Kubota-Okamoto S, Usui R, Ishitobi M, Yamazaki Y, Hamamoto Y, Kurose T, Seino Y, Yamada Y, Seino Y (2021) Effects of glucagon-like peptide-1 receptor agonists on secretions of insulin and glucagon and gastric emptying in Japanese individuals with type 2 diabetes: a prospective, observational study. J Diabetes Investig 12: 2162–2171.

Levdik TI (1989) [Unification of the staining of histological preparations and histoautoradiograms with Harris hematoxylin]. Arkh Patol 51: 81–82.

Li J, Liu H, Shang L (2023) Tert-butylhydroquinone mitigates renal dysfunction in pregnant diabetic rats via attenuation of oxidative stress and modulation of the iNOs/ NFκB/TNF alpha signalling pathway. Endocr Metab Immune Disord Drug Targets 23: 633–646.

Maranta F, Cianfanelli L, Cianflone D (2021) Glycaemic control and vascular complications in siabetes mellitus type 2. Adv Exp Med Biol 1307: 129–152.

Miric G, Dallemagne C, Endre Z, Margolin S, Taylor SM, Brown L (2001) Reversal of cardiac and renal fibrosis by pirfenidone and spironolactone in streptozotocin-diabetic rats. Br J Pharmacol 133: 687–694.

Moustafa Ahmed Y, Shehata Messiha BA, El-Sayed El-Daly M, Abo-Saif AA (2019) Effects of ticagrelor, empagliflozin and tamoxifen against experimentally-induced vascular reactivity defects in rats in vivo and in vitro. Pharmacol Rep 71: 1034–1043.

Nankar SA,Bulani Y,Sharma SS and Pande AH (2020) ApoE-Derived Peptides Attenuated Diabetes-Induced Oxidative Stress and Inflammation. Protein Pept Lett 27(3): 193-200.

Patel S and Santani D (2009) Role of NF-kappa B in the pathogenesis of diabetes and its associated complications. Pharmacol Rep 61(4): 595-603.

Reed MJ, Meszaros K, Entes LJ, Claypool MD, Pinkett JG, Gadbois TM, Reaven GM (2000) A new rat model of type 2 diabetes: the fat-fed, streptozotocin-treated rat. Metabolism 49: 1390–1394.

Rojas-Carranza CA, Bustos-Cruz RH, Pino-Pinzon CJ, Ariza-Marquez YV, Gomez-Bello RM, Canadas-Garre M (2018) Diabetes-related neurological implications and pharmacogenomics. Curr Pharm Des 24: 1695–1710.

Rufino M, Barbero P, Hernandez D, Torres A, Lorenzo V (2007) [Usefulness of oral glucose tolerance test (OGTT) in output patients with advanced chronic renal failure (CRF)]. Nefrologia 27: 30–37.

Schirmeister J, Willmann H, Kiefer H (1964) [Plasma creatinine as rough indicator of renal function]. Dtsch Med Wochenschr 89: 1018–1023.

Sethi S, D'Agati VD, Nast CC, Fogo AB, De Vriese AS, Markowitz GS, Glassock RJ, Fervenza FC, Seshan SV, Rule A, Racusen LC, Radhakrishnan J, Winearls CG, Appel GB, Bajema IM, Chang A, Colvin RB, Cook HT, Hariharan S, Herrera Hernandez LP, Kambham N, Mengel M, Nath KA, Rennke HG, Ronco P, Rovin BH, Haas M (2017) A proposal for standardized grading of chronic changes in native kidney biopsy specimens. Kidney Int 91: 787–789.

Seufert J and Gallwitz B (2014) The extra-pancreatic effects of GLP-1 receptor agonists: a focus on the cardiovascular, gastrointestinal and central nervous systems. Diabetes Obes Metab 16: 673–688.

Sleem M, Taye A, El-Moselhy MA, Mangoura SA (2014) Combination therapy with losartan and L-carnitine protects against endothelial dysfunction of streptozotocin-induced diabetic rats. Eur J Pharmacol 744: 10–17.

Song F, Jia W, Yao Y, Hu Y, Lei L, Lin J, Sun X, Liu L (2007) Oxidative stress, antioxidant status and DNA damage in patients with impaired glucose regulation and newly diagnosed Type 2 diabetes. Clin Sci (Lond) 112: 599–606.

Song Y, Liu W, Tang K, Zang J, Li D, Gao H (2020) Mangiferin alleviates renal interstitial fibrosis in streptozotocin-induced diabetic mice through regulating the PTEN/PI3K/Akt signaling pathway. J Diabetes Res 2020: 9481720.

Taylor CR, Burns J (1974) The demonstration of plasma cells and other immunoglobulin-containing cells in formalin-fixed, paraffin-embedded tissues using peroxidase-labelled antibody. J Clin Pathol 27: 14–20.

Towbin H, Staehelin T, Gordon J (1979) Electrophoretic transfer of proteins from polyacrylamide gels to nitrocellulose sheets: procedure and some applications. Proc Natl Acad Sci 76: 4350–4354.

Vincent AM, Callaghan BC, Smith AL, Feldman EL (2011) Diabetic neuropathy: cellular mechanisms as therapeutic targets. Nat Rev Neurol 7: 573–583.

Wang P, Yang Y, Wang D, Yang Q, Wan J, Liu S, Zhou P, Yang Y (2020) Cinnamaldehyde ameliorates vascular dysfunction in diabetic mice by activating Nrf2. Am J Hypertens 33: 610–619.

Wang S, Abouzied M, Smith D (1996) Proteins as potential endpoint temperature indicators for ground beef patties. J Food Sci 61: 5–7.

Wang W, Shang C, Zhang W, Jin Z, Yao F, He Y, Wang B, Li Y, Zhang J, Lin R (2019) Hydroxytyrosol NO regulates oxidative stress and NO production through SIRT1 in diabetic mice and vascular endothelial cells. Phytomedicine 52: 206–215.

Wang X, Han X, Li M, Han Y, Zhang Y, Zhao S, Li Y (2018) Ticagrelor protects against AngII-induced endothelial dysfunction by alleviating endoplasmic reticulum stress. Microvasc Res 119: 98–104.

Wilcox AA, Carroll WE, Sterling RE, Davis HA, Ware AG (196) Use of the Berthelot reaction in the the automated analysis of serum urea nitrogen. Clin Chem 12: 151–157.

Wohlfart P, Linz W, Hubschle T, Linz D, Huber J, Hess S, Crowther D, Werner U, Ruetten H (2013) Cardioprotective effects of lixisenatide in rat myocardial ischemia-reperfusion injury studies. J Transl Med 11: 84.

Xiao M, Lu D, Tian J, Yu Y, Zhang Q, Zhang L, Chang D (2020) The protective effects of GLP-1 receptor agonist lixisenatide on oxygen-glucose deprivation/reperfusion (OGD/R)-induced deregulation of endothelial tube formation. RSC Adv 10: 10245–10253.

Yamagishi S, Fukami K, Ueda S, Okuda S (2007) Molecular mechanisms of diabetic nephropathy and its therapeutic intervention. Curr Drug Targets 8: 952–959.

Yamagishi S, Nakamura K, Matsui T, Noda Y, Imaizumi T (2008) Receptor for advanced glycation end products (RAGE): a novel therapeutic target for diabetic vascular complication. Curr Pharm Des 14: 487–495.

Yamagishi SI (2019) Role of advanced glycation endproduct (AGE)-receptor for advanced glycation endproduct (RAGE) axis in cardiovascular disease and its therapeutic intervention. Circ J 83: 1822–1828.

Ye Y, Birnbaum GD, Perez-Polo JR, Nanhwan MK, Nylander S, Birnbaum Y (2015) Ticagrelor protects the heart against reperfusion injury and improves remodeling after myocardial infarction. Arterioscler Thromb Vasc Biol 35: 1805–1814.

Yuchen C, Hejia Z, Fanke M, Qixin D, Liyang C, Xi G, Yanxia C, Xiongyi Y, Zhuohang X, Guoguo Y , Min F (2023) Exploring the shared molecular mechanism of microvascular and macrovascular complications in diabetes: Seeking the hub of circulatory system injury. Front Endocrinol 14: 1032015.

Zhang L, Huang YJ, Sun JP, Zhang TY, Liu TL, Ke B, Shi XF, Li H, Zhang GP, Ye ZY, Hu J, Qin J (2021) Protective effects of calorie restriction on insulin resistance and islet function in STZ-induced type 2 diabetes rats. Nutr Metab (Lond) 18: 48.

Zhao H, Wu L, Yan G, Chen Y, Zhou M, Wu Y, Li Y (2021) Inflammation and tumor progression: signaling pathways and targeted intervention. Signal Transduct Target Ther 6: 263.

Zhao Q, Xu H, Zhang L, Liu L, Wang L (2019) GLP-1 receptor agonist lixisenatide protects against high free fatty acids-induced oxidative stress and inflammatory response. Artif Cells Nanomed Biotechnol 47: 2325–2332.

Zhou B, Chen Y, Yuan H, Wang T, Feng J, Li M, Liu J (2021) NOX1/4 Inhibitor GKT-137831 improves erectile function in diabetic rats by ROS reduction and endothelial nitric oxide synthase reconstitution. J Sex Med 18: 1970–1983.

Zhou SJ, Bai L, Lv L, Chen R, Li CJ, Liu XY, Yu DM, Yu P (2014) Liraglutide ameliorates renal injury in streptozotocin-induced diabetic rats by activating endothelial nitric oxide synthase activity via the downregulation of the nuclear factor-kappaB pathway. Mol Med Rep 10: 2587–2594.

Zhou Z, Zhong J, Zhang J, Yang J, Leng X, Yao B, Wang X, Dong H (2023) Comparative transcriptome analysis provides insight into the molecular targets and signaling pathways of deer TGF-1 regulating chondrocytes proliferation and differentiation. Mol Biol Rep 50: 3155–3166.